



HAL
open science

Mapping Beaufort Sea Topography and Geophysical Settings Using High-Resolution Geospatial Data and GMT

Polina Lemenkova

► **To cite this version:**

Polina Lemenkova. Mapping Beaufort Sea Topography and Geophysical Settings Using High-Resolution Geospatial Data and GMT. *Geografické informácie*, 2020, 24 (1), pp.4-18. 10.17846/GI.2020.24.1.4-18 . hal-02916437

HAL Id: hal-02916437

<https://hal.science/hal-02916437>

Submitted on 25 Sep 2020

HAL is a multi-disciplinary open access archive for the deposit and dissemination of scientific research documents, whether they are published or not. The documents may come from teaching and research institutions in France or abroad, or from public or private research centers.

L'archive ouverte pluridisciplinaire **HAL**, est destinée au dépôt et à la diffusion de documents scientifiques de niveau recherche, publiés ou non, émanant des établissements d'enseignement et de recherche français ou étrangers, des laboratoires publics ou privés.



Distributed under a Creative Commons Attribution 4.0 International License

MAPPING BEAUFORT SEA TOPOGRAPHY AND GEOPHYSICAL SETTINGS USING HIGH-RESOLUTION GEOSPATIAL DATA AND GMT

Polina Lemenkova

Abstract

The papers presents an integrated processing of the high-resolution thematic data covering the area of the Beaufort Sea, a marginal sea of the Arctic Ocean, northern Canada and Alaska. Five thematic maps of the Beaufort Sea, Arctic Ocean are presented. The cartographic techniques were performed by Generic Mapping Tools (GMT) scripting toolset. The methodology presents the integration of the multi-source high-resolution thematic datasets: bathymetric GEBCO, IBCAO, topographic GLOBE, sediment thickness GlobSed, EGM2008 geoid model, GMT vector layers and geophysical gravity model from CryoSat-2 and Jason-1. There is an agreement with the data by their inspection and analysis of grids correlation. The bathymetric map demonstrated variations in depths with rapidly decreasing values in the Mackenzie River coasts, depicting the basin of the Beaufort Sea, large shelf in the Canadian Arctic Archipelago and western part bordering the Chukchi Sea. The GDAL inspection shows that the GEBCO-based topography ranges between -3,973 m to 2,578 m. Gravity data shows that coastal areas in northern Canada and Alaska have values >20 mGal while the basin of the Beaufort Sea is dominated by the lower values at -65 to -45 mGal; the data range is from -155.097 to 366.939 mGal. The marine free-air gravity fields and geoid data demonstrate correlation with topographic isolines of the region. The data range for the sediment thickness is from 0.00 to 18064.53 m having maximal data at the Mackenzie River discharge area. A comprehensive compilation of the data on the Beaufort Sea visualized using GMT presents more insights into its bathymetric structure and geophysical fields distribution in context of the variability of the geological settings.

Keywords: Beaufort Sea, Arctic Ocean, GMT, cartography, data integration

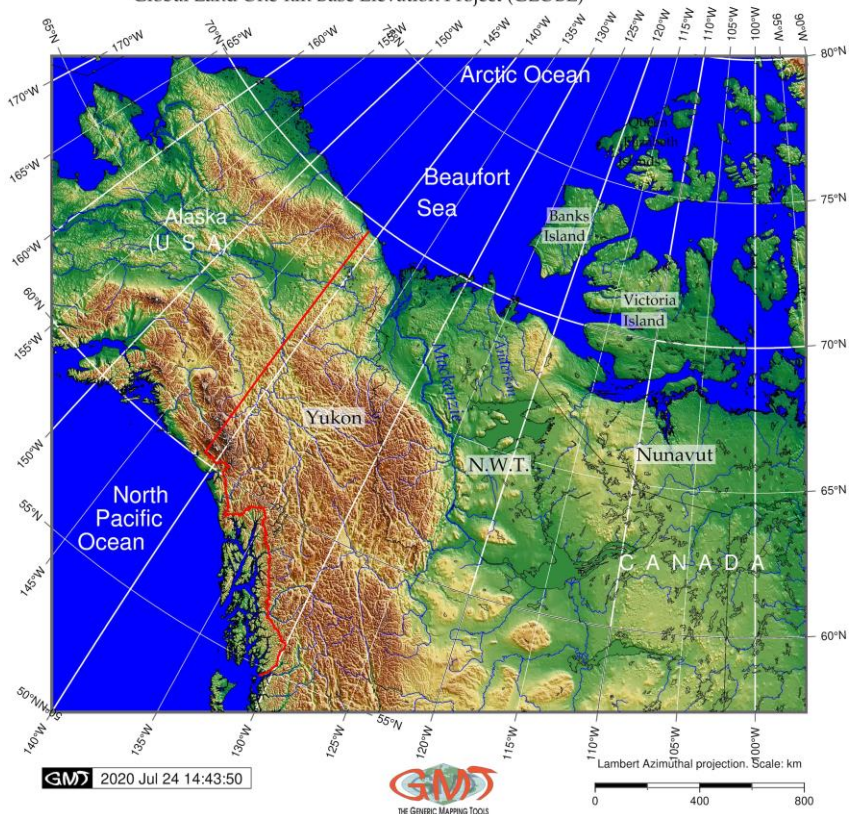
Introduction

The study object is the Beaufort Sea, a marginal sea of the Arctic Ocean, located west off the Canadian Arctic Archipelago and north off Alaska (Map 1). The topography of the Beaufort Sea varies in its different part in northern Canada and the U. S. A narrow strip of the coastal area has rather shallower depths (<60 m) increasing northwards to a few kilometers. Especially shallow areas can be noted between 180°W and 160°W in the western part of the sea and in the areas between

numerous islands of the Canadian Archipelago. However, the central part of the open areas of the sea (purple-colored areas on Map 2) is presented by a large massive platform, similar to an open ocean basin, which can be noted on Map 2. In general, the shelf of the Beaufort Sea is much narrower comparing to other shelf areas of the Arctic Basin. Specifically, off the coast of Alaska the shelf stretches along the mainland's bedrock. In the eastern area it continues off the northern coast of Canada among numerous islands of the Canadian Arctic Archipelago.

Map 1: Topographic map of the Northern Canada and the U.S. Alaska based on GLOBE. Source: author.

Topographic map of the Northern Canada and Alaska based on GLOBE DEM
GLOBE 30-arc-second (1-km) gridded DEM, Version 1.0
Global Land One-km Base Elevation Project (GLOBE)



The geological perspectives of the Beaufort Sea exploration is explained by the mineral resources and reserves of its shelf area including oil and natural gas (Ayles et al., 2002). However, the discoveries of the drilled offshore wells in the Mackenzie Delta and beneath the seafloor mostly remain undeveloped among other Arctic Seas, e.g. the Sverdrup Basin, and offshore Alaska (Gautier et al., 2009). The geological structure of the seafloor in the Canadian Archipelago region can be briefly characterized as follows. The crystalline basement surface has uplifts where numerous islands are located. Various local depressions on the seafloor with depths of several kilometers are stretching between a series of faults. The most extensive depressions in the Canadian Arctic are occupied by the Hudson Bay, the Baffin Bay and the Beaufort Sea. The basin of the Beaufort Sea is rather large in size, merging with the basin of the Chukchi Sea in the west (Mahoney et al., 2014). Most of its seafloor bottom is occupied by an abyssal plain with depths at 3800 m.

The geomorphology of the seafloor relief is notable by a narrow shelf that quickly drops off into deeper water and complicated by numerous submarine valleys. The coastal shelf area is narrow, especially near the Alaska. The main source of the sediment inflow is presented by the Mackenzie River, which is the longest river in Canada, entering the Beaufort Sea (Stein, 2008). The climate of the Beaufort Sea is rather severe frozen over the most of the year. As discussed above and assessed previously (Usher, 2002; Ayles and Snow, 2002), the Beaufort Sea has a potential in mineral resources and environmental significance (Cobb et al. 2014; Barnes et al. 1984) which explains the actuality of its studies based on the high-resolution data and advanced cartographic visualization, such as GMT.

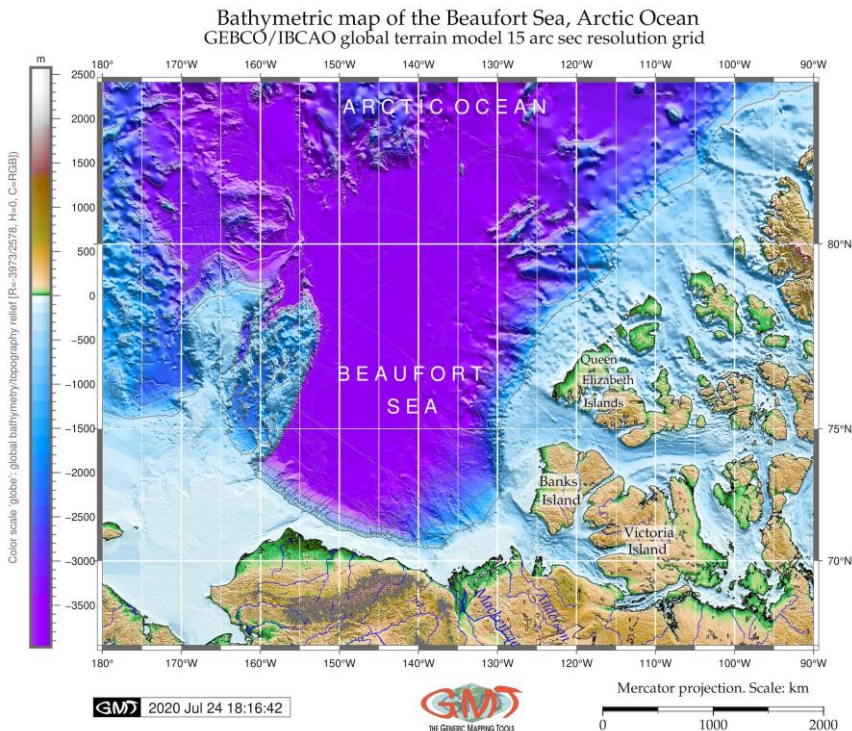
Geospatial data

The importance of the geodata for quality and precision of the cartographic mapping has been discussed (Smith, 1993; Gauger et al. 2007; Lemenkova, 2019a, 2020a). Therefore, the data were taken from a variety of the reliable sources and included high-resolution raster grids and vector layers selected as the input raw data. The origin of the topographic map (Map 1) is the GLOBE 30-arc-second (1-km) gridded, global DEM with the horizontal coordinate system presented as seconds of lat/lon referenced to WGS84. The GLOBE has been developed by the GLOBE Task Team, created by the Committee on Earth Observation Satellites (CEOS), NOAA (Hastings et al., 1999) with detailed technical cartographic documentation presented by Hastings and Dunbar (1999). The coastal land areas, shore lines, borders of rivers and national continents were derived from the GMT-embedded vector layers (Wessel & Smith, 1996).

The bathymetric maps of the seafloor and marine areas (Map 2) was visualized based on the 15-arc-second General Bathymetric Chart of the Oceans (GEBCO) developed by GEBCO Compilation Group (2020) and its regional

implementation International Bathymetric Chart of the Arctic Ocean (IBCAO) developed by Jakobsson et al. (2008, 2012).

Map 2: Bathymetric map of the Beaufort Sea basin, Arctic. Source: author.



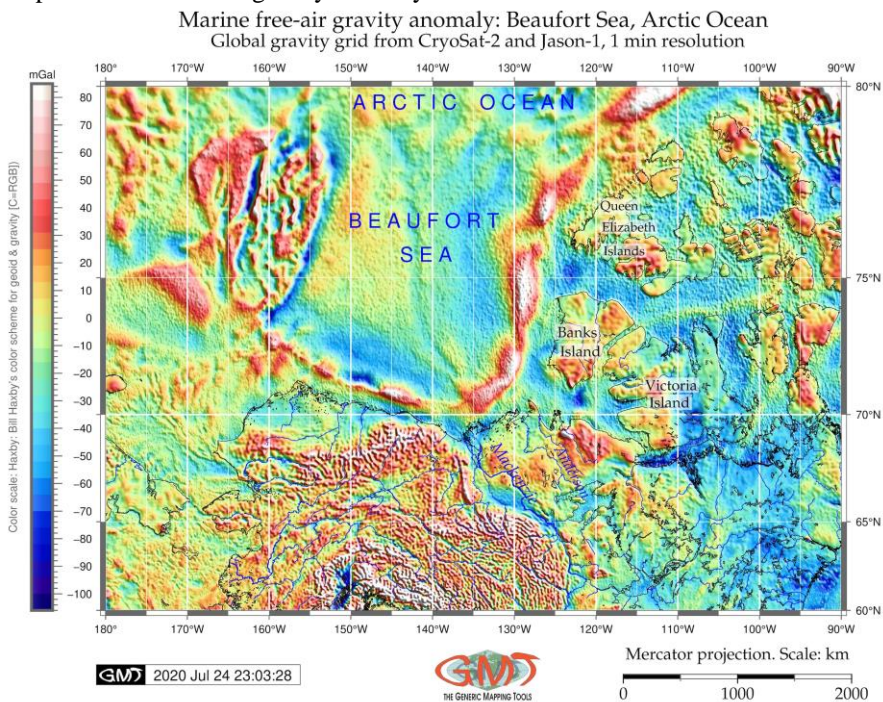
The marine gravity model (Map 3) is taken from the raster grids at Scripps Institution of Oceanography (SIO) which are public domain raster grids of the marine gravity anomalies computed from CryoSat-2 and Jason-1 (Sandwell et al., 2014). The model showing geoid undulations (Map 4) was based on the Earth Gravitational Model 2008 (Pavlis et al., 2012). The sediment thickness (Map 5) is based on the 5-minute resolution data grid from NOAA by the World Data Service for Geophysics (Straume et al., 2019).

Theoretical-methodical background of GMT

The research has been technically done using the Generic Mapping Tools (GMT) scripting toolset, which is an alternative way of cartographic tools

comparing to the traditional GIS, e.g. ArcGIS widely used in geosciences (Suetova et al. 2005a, 2005b; Klaučo et al., 2014, 2017; Lemenkova et al., 2012; Kuhn et al. 2006). The fundamental difference between the GIS and GMT consists in its console-based approach of mapping and absence of the classic menu-based Graphical User's Interface (GUI), which is technically described in the existent works (Lemenkova, 2019b, 2019c).

Map 3: Marine free-air gravity anomaly in the Beaufort Sea. Source: author.

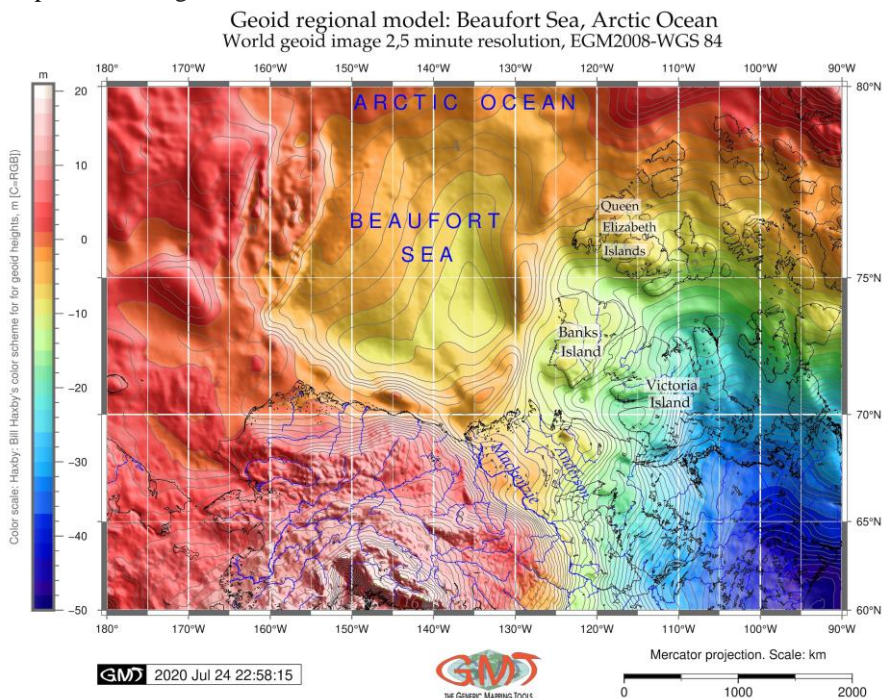


A GMT has been developed by Paul Wessel and Walter H. F. Smith in 1988, officially releasing in 1991 (Wessel and Smith, 1991) and is being actively and continuously developed since then (Wessel et al., 2013). The scripting methods of GMT provide a high degree of automatization in a cartographic work which increases both the quality and the precision of mapping due to the machine learning approach which is progressively applied in geosciences (e.g. Schenke and Lemenkova, 2008; Lemenkova, 2019e, 2019f).

GMT modules and scripting approach

The main approach of GMT consists in subdivision of the cartographic script into several tasks, where every task is being made using a special module. For instance, a visualization of the GEBCO grid was done using a module ‘grdimage’ by a code: ‘gmt grdimage GEBCO_2019.nc -Cmyocean.cpt -R180/270/66/83 -JM5.5i -P -I+a15+ne0.75 -Xc -K > \$ps’. Within a code, the ‘GEBCO_2019.nc’ is the name of the file. The color palette was made using ‘makecpt’ module by this code: gmt makecpt -Cglobe.cpt -V -T-3973/2578 > myocean.cpt. Here, the existing color palette ‘globe’ was stretched to the actual z-range of this map (that is, minimal depth is -3973 m, maximal elevation is 2578 m). The same principle of the GMT syntax is explained in more details (Lemenkova, 2019d, 2020c).

Map 4: Geoid regional model of the Beaufort Sea basin. Source: author.

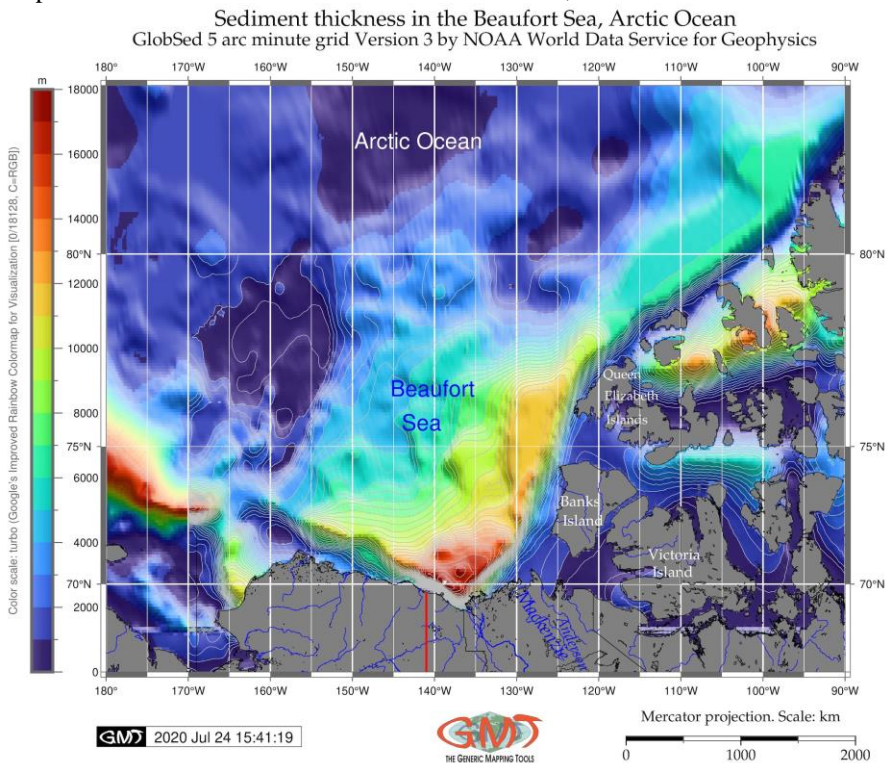


Data format conversion and inspection

Plotting GLOBE grid (Map 1) requires some additional explanation. Because the original data were in gridded binary files with the elevation stored as 16-bit signed

integer numbers, the initial step consisted in converting this file to the ‘xyz’ format, that is, a GMT *.grd extension. The conversion was done using a GMT module ‘xyz2grd’ by the following code: ‘xyz2grd a10g -Ga10GLOBE.grd -R-180/-90/50/90 -I30c -N-9999 -V -F -ZTLh’. As a result, the original file ‘a10g’ from the GLOBE tiles was converted to a GMT file with a .grd extension ‘a10GLOBE.grd’. The actual range of the topographic elevations was checked up by the Geospatial Data Abstraction Library (GDAL), a library supporting various tasks in processing spatial datasets (GDAL/OGR contributors 2020).

Map 5: Sediment thickness in the Beaufort Sea basin, Arctic. Source: author.



GDAL handles raster data by supporting ca. 100 raster formats. A gdalinfo utility of GDAL was applied using the code ‘gdalinfo grid_textGLOBE.grd -stats’ to check up the data range. The GLOBE is a topographic grid (without detailed bathymetry), therefore, the actual z-data are noted as actual_range={-500,6098}. The visualization is done using a ‘grdimage’ GMT module. The script was made

using a combination of the GMT modules (grdimage, psscale, grdcontour, psbasemap, pscoast, pstext, gmtlogo, psconvert) by the principle explained above.

Cartographic projections

Cartographic projections were set up by the 'grdimage' module. The topographic map (Map 1) was plotted using Lambert Azimuthal projection which was set up using commands '-R220/50/270/80r' (here, small 'r' letter means that the extent of the map is specified by the lower left and upper right coordinates) and then '-JA260/60/5.5i', which defines the standard meridian and parallel of the coordinate grid and layout extension (5.5 inches). For other maps, the '-R180/270/66/83' flag means selected region with coordinates in WESN convention, the '-JM5.5i' flag means visualizing a map in Mercator projection. The extents of the geophysical maps (Map 3 and Map 4) are given until 80°N due to the original limits of the raw data.

Data interpolation

The map of the sediment thickness (Map 5) was visualized using the GlobSed original grid by GMT. The continuous field of the sediment thickness was plotted using the interpolation technique, to estimate the values at the locations where direct observations are not available. The existing locations of the original grid GlobSed has an accurate measure at the 5 arc-minute resolution with each node as an observation point of the sediment thickness. Knowing the coordinates and values of the sediment thickness, these data were interpolated using 'grdcontour' module: 'gmt grdcontour cs_sed.nc -R -J -C500 -Wthinnest,gray -O -K >> \$ps'. Here, the isolines were plotted via every 500 m showing the continuous field. Using this technique, the unknown values of the sediments at other locations were estimated and isolines plotted. An advantage of the interpolation technique consists in the visualized isolines on the thematic maps where a set of contour lines is plotted to connect locations with the same values (e.g. topographic and bathymetric showing elevation, marine free-air gravity maps and geoid).

Results of the data correlation and comparative analysis

The compiled visualization of the several thematic datasets attempts to determine the structural trends in the central basin of the Beaufort Sea. The integration of data on topography, bathymetry, marine free-air gravity and geoid shows that gravity anomalies correlate with geological lineaments, crustal structure, and seismicity at the subduction zones of the tectonic plates, which is supported by previous studies (Bassett and Watts, 2015).

Gravity data has been used for cartographic modelling showing main field trends of the study area: the coastal areas of the northern Canada and Alaska have

values above 20 mGal (orange to red colored areas on Map 3) while the basin of the Beaufort Sea is dominated by the lower values at -65 to -45 mGal (blue colored, Map 3) and -45 to 15 (cyan to light green areas, Map 3). Selected areas have slightly positive values from 0 to 20 mGal (yellow colors, Map 3). Comparing the bathymetric map with the marine free-air gravity and geoid (Map 2 to 3 and 4) one can see that the isolines of the shelf areas of the Beaufort Sea are corresponding to those of the geoid and gravity fields depicting the basin of the sea. According to the GDAL check (gdalinfo bs_relief.nc -stats), the bathymetry and topography in the study area ranges between -3,973 m to 2,578 m.

The map of the geoid undulations of the Beaufort Sea (Map 4) shows that central part of the sea has values at -10 to 5 m contrasting with the southeastern part of the study area (blue-colored region southward off Victoria Island in the Canada Archipelago). Values of geoid undulations show the distance between the geoid and ellipsoid where the geoid is a model of the global mean sea level to measure precise Earth's surface elevations analyzed to determine the depth to the basement surface.

The values obtained from the gravity data control points in the gravity modelling (EGM2008). The comparison of the relief map from topographic data, gravity and geoid models and sediment thickness has been performed. The depths at the Beaufort Sea rapidly increase from the shelf areas northwards (open Arctic Ocean). Besides, a large shelf areas can be seen on the west part of the study area (northward of Alaska) and in the eastern areas between the islands of the Canadian Archipelago. The sedimentary cover has a thickness at about 1.5–2 km in the southern part and increases to more than 4 km in the northeastern and western parts and changes gradually in the other parts of the study area. The total data range lies between 0 (no sediments) to 18,064 m (very thick layer) in the southern shelf areas near the mouth of the Mackenzie River, according to the GDAL data inspection of the NetCDF file (gdalinfo bs_sed.nc -stats).

The results of the structural trend analysis indicate that study area is greatly affected by the two structural trends: 1) 'south–north' indicates shelf areas contrasting to the open Arctic Ocean; 2) 'east–center–west' trend indicates contrasting areas of shelf northward of Alaska, central part of the basin and Canadian Archipelago. These trends are associated with the topographic variations of the sea that in turn are caused by the geologic structure of the underlying rocks that build it (lithology, facies, age) and specifics of the regional tectonics, including faults and lineaments, out-of-sequence dislocations, and thrusts (Lemenkova, 2020b, 2018).

The 'south–north' and 'east–center–west' topographic subdivisions can be traced on the topographic and bathymetric maps (Map 1 and Map 2). Topographically, this region presents a highly fragmented continental margin. The islands of the Canadian Arctic Archipelago are presented by the uplifted blocks.

The straits between the islands correspond to the zones of linear deflections limited by faults.

The dominating directions of the topographic trends are meridional and latitudinal strikes of the local minor troughs and straits. The transverse troughs formed by straits and large fjords dissect the outer shelf of the Canadian Arctic Archipelago in a number of the shallow banks where depths are less than 200 m, while depths in the troughs may reach up to 300-500 m (Map 2). The connection of the topography with geological structure can be illustrated by the crystalline basement surface in the Canadian Arctic Archipelago which has a stepped-block topography formed by the uplifts where numerous islands and their structural cores are located. Other topographic forms include depressions along a series of faults where depths reach up to several kilometers. The depression in the Beaufort Sea is rather large in size, bordering the basin of the Chukchi Sea.

The analysis of the thematic maps of the Beaufort Sea shows general distribution of the geophysical patterns according to their shape and amplitude and trends of the gravity and geoid anomalies in the Canadian Arctic Archipelago. The character of data distribution in the marine free-air gravity anomaly zones (Map 3), geoid undulations (Map 4) and bathymetry (Map 2) mirrors geological variations in the crystalline basement structure and rocks properties beneath the seafloor. The sediment thickness shows clear correlation with the shelf area in general: higher values are dominating near the coast and especially Mackenzie River, and, on the contrary, lower values are notable in the open sea (Map 5).

Conclusion

A comprehensive compilation of the data on the Beaufort Sea visualized using the GMT toolset presents more insights into its topographic structure and distribution of the geophysical fields in context of the variability of the geological settings. An integrated multi-source thematic raster data including GEBCO, GLOBE, EGM2008, IBCAO, GlobSed and marine free-air gravity anomalies has not been available yet in the existing literature. This paper aimed to fill in this gap by presenting the possibilities of the data integration using scripting technologies of GMT for visualizations of one of the Arctic Ocean regions, the Beaufort Sea.

The GMT-based interpretation of the map series (topography, bathymetry, geophysical grids of gravity and geoid, geology, sediment thickness) included qualitative cartographic analysis of their isolines, inspection of the geometric forms of the geoid fields and trends in marine free-air gravity anomalies over the region of the Beaufort Sea. The links between the different variables, visualized on the maps, allow to perform a complex analysis and find new correlations in a spatial analysis. Thus, the identification of the linear trends and isolines enables to find out a correlation between the features of the geophysical phenomena (Grant &

West, 1990): geographic locations and amplitudes of positive and negative values within the datasets (GDAL), topographic patterns, regional extent of the isolines, amplitude of the anomalies (marked by color palettes in the geoid or gravity grids).

A hybrid use of the thematic datasets of raster and vector formats are used using the GMT scripting toolset. The advantage of the GMT over the traditional GIS, such as MapInfo, ArcGIS, QGIS or programming approaches (e.g. Klaučo et al. 2013; Lemenkova, 2020d) consists in its relational and flexible approach to the data handling: a GMT based mapping does not require creating a GIS-project or operating with GUI. In contrast, all the maps can be plotted using a shell script. The GMT handles both types of formats (vector or raster) and is very useful in a project with rapidly changing cartographic demands: projections, map extent, adding new elements on a layout, modifying graphical elements: transparency, fonts, symbols, converting data formats, queries via GDAL, plotting complex legends, automatic adding a time stamp of map production, to mention a few.

Besides cartographic flexibility and open access, the scripting approach of the GMT increases automatization of the mapping, the degree of machine learning instead of handmade routine, speed and precision of mapping. The elements plotted on a map are stored in a script using a GMT syntax. The scripting principle allows to reuse the codes applied for a new map by adding variables into the code lines and changing a regional extent. The integrated solution for the data handling by GMT acts as a gateway between the multi-source data, format conversion and visualization output. This paper demonstrated handling of high-resolution data from different sources and origins processed by GMT and presented as a series of maps: GEBCO, IBCAO, GLOBE, GlobSed, EGM2008, GMT vector layers and gravity model from CryoSat-2 and Jason-1. Combining such diverse datasets was made possible on a regional scale (the Beaufort Sea, northern Canada and Alaska) through the subset of AOI from the global grids and reformatting the original formats to a NetCDF, compatible with GMT. Besides data aggregation, technical possibilities of GMT accelerated cartographic workflow through automatization and simplified the process of data extraction and visualization of geoinformation.

References

- AYLES, G. B. – BELL, R. – FAST, H. 2002. The Beaufort Sea Conference 2000 on the renewable marine resources of the Canadian Beaufort Sea. In *Arctic*. 2002, vol. 55, pp. 3-5.
- AYLES, B. – SNOW, N. 2002. Canadian Beaufort Sea: the environmental and social setting. In *Arctic*. 2002, vol. 55, no. 1, pp. 4-17.
- BASSETT, D. – WATTS, A. B. 2015. Gravity anomalies, crustal structure, and

- seismicity at subduction zones: 1. Seafloor roughness and subducting relief. In *Geochemistry, Geophysics, Geosystem*. 2015, vol. 16, no. 5, pp. 1508-1540.
- BARNES, P. W. – SCHELL, D. M. – REIMNITZ, E. 1984. *The Alaskan Beaufort Sea. Ecosystems and Environments*. Elsevier: Academic Press, 1984. 482 p. ISBN 978-0-12-079030-2.
- COBB, D. G. – ROY, V. – LINK, H. – ARCHAMBAULT, P. 2014. Information to support the reassessment of ecologically and biologically significant areas (EBSAs) in the Beaufort Sea Large Ocean Management Area. [online]. In *Canadian Science Advisory Secretariat (CSAS)*, Research Document 2014/097. 37 p. ISSN 1919-5044. Available on the Internet: <http://www.dfo-mpo.gc.ca/csas-sccs/publications/resdocs-docrech/2014/2014_097-eng.html>
- GAUGER, S. – KUHN, G. – GOHL, K. – FEIGL, T. – LEMENKOVA, P. – HILLENBRAND, C. 2007. Swath-bathymetric mapping. In *Reports on Polar and Marine Research*. 2007, vol. 557, pp. 38-45.
- GAUTIER, D. L. – BIRD, K. J. – CHARPENTIER, R. R. – GRANTZ, A. – HOUSEKNECHT, D. W. – KLETT, T. R. – MOORE, T. E. – PITMAN, J. K. – SCHENK, C. J. – SCHUENEMEYER, J. H. – SORENSEN, K. – TENNYSON, M. E. – VALIN, Z. C. – WANDREY, C. J. 2009. Assessment of undiscovered oil and gas in the Arctic. In *Science*. 2009, vol. 324, pp. 1175-1179.
- GEBCO Compilation Group 2020. GEBCO 2020 Grid. DOI: 10.5285/a29c5465-b138-234d-e053-6c86abc040b9
- GDAL/OGR contributors 2020. GDAL/OGR Geospatial Data Abstraction software Library. [online]. Open Source Geospatial Foundation. Available on the Internet: <<https://gdal.org>>
- GRANT, F. – WEST, G. 1990. *Interpretation Theory in Applied Geophysics*. New York: McGraw-Hill, 1990. 584 p. ISBN 978-0-07024-100-8
- HASTINGS, D. A. – DUNBAR, P. K. 1999. *Global Land One-kilometer Base Elevation (GLOBE) Digital Elevation Model, Documentation, Volume 1.0*. [online]. Key to Geophysical Records Documentation (KGRD) 34. National Oceanic and Atmospheric Administration, National Geophysical Data Center, 325 Broadway, Boulder, Colorado 80303, U.S.A. Available on the Internet: <<https://www.ngdc.noaa.gov/mgg/topo/report/globedocumentationmanual.pdf>>
- HASTINGS, D. A. – DUNBAR, P. K. – ELPHINSTONE, G. M. – BOOTZ, M. – MURAKAMI, H. – MARUYAMA, H. – MASAHARU, H. – HOLLAND, P. – PAYNE, J. – BRYANT, N. A. – LOGAN, T. L. – MULLER, J.-P. – SCHREIER, G. – MACDONALD, J. S. 1999. *The Global Land One-kilometer Base Elevation (GLOBE) Digital Elevation Model, Version 1.0*. [online]. NOAA, National Geophysical Data Center, 325 Broadway, Boulder, Colorado 80303, U.S.A. Available on the Internet: <<http://www.ngdc.noaa.gov/mgg/topo/globe.html>>

- JAKOBSSON, M. – MACNAB, R. – MAYER, L. – ANDERSON, R. – EDWARDS, M. – HATZKY, J. – SCHENKE, H. W. – JOHNSON, P. 2008. An improved bathymetric portrayal of the Arctic Ocean: Implications for ocean modeling and geological, geophysical and oceanographic analyses. In *Geophysical Research Letters*. 2008, vol. 35, no. 7, pp. 1-5. DOI: 10.1029/2008GL033520.
- JAKOBSSON, M. – MAYER, L. A. – COAKLEY, B. – DOWDESWELL, J. A. – FORBES, S. – FRIDMAN, B. – HODNESDAL, H. – NOORMETS, R. – PEDERSEN, R. – REBESCO, M. – SCHENKE, H.-W. – ZARAYSKAYA Y. – ACCETTELLA, D. M – ARMSTRONG, A. – ANDERSON, R. M. – BIENHOFF, P. – CAMERLENGHI, A. – CHURCH, I. – EDWARDS, M. – GARDNER, J. V. – HALL, J. K. – HELL, B. – HESTVIK, O. B. – KRISTOFFERSEN, Y. – MARCUSSEN, C. – MOHAMMAD, R. – MOSHER, D. – NGHIEM, S. V. – PEDROSA, M. T. – TRAVAGLINI, P. G. – WEATHERALL, P. 2012. The International Bathymetric Chart of the Arctic Ocean (IBCAO) Version 3.0. In *Geophysical Research Letters*. 2012, vol. 39, no. L12609, pp. 1-6. DOI: 10.1029/2012GL052219.
- KLAUČO, M. – GREGOROVÁ, B. – STANKOV, U. – MARKOVIĆ, V. – LEMENKOVA, P. 2013. Determination of ecological significance based on geostatistical assessment: a case study from the Slovak Natura 2000 protected area. In *Central European Journal of Geosciences*. 2013, vol. 5, no. 1, pp. 28-42.
- KLAUČO, M. – GREGOROVÁ, B. – STANKOV, U. – MARKOVIĆ, V. – LEMENKOVA, P. 2014. Landscape metrics as indicator for ecological significance: assessment of Sitno Natura 2000 sites, Slovakia. In *Ecology and Environmental Protection. Proceedings of the International Conference*. 2014, pp. 85-90.
- KLAUČO, M. – GREGOROVÁ, B. – STANKOV, U. – MARKOVIĆ, V. – LEMENKOVA, P. 2017. Land planning as a support for sustainable development based on tourism: A case study of Slovak Rural Region. In *Environmental Engineering and Management Journal*. 2017, vol. 2, no. 16, pp. 449-458.
- KUHN, G. – HASS, C. – KOBER, M. – PETITAT, M. – FEIGL, T. – HILLENBRAND, C. D. – KRUGER, S. – FORWICK, M. – GAUGER, S. – LEMENKOVA, P. 2006. The response of quaternary climatic cycles in the South-East Pacific: development of the opal belt and dynamics behavior of the West Antarctic ice sheet. In *Expeditionsprogramm Nr. 75 ANT XXIII/4*. Bremerhaven: AWI, 2006. 49 p.
- LEMENKOVA, P. 2020a. Visualization of the geophysical settings in the Philippine Sea margins by means of GMT and ISC data. In *Central European Journal of Geography and Sustainable Development*. 2020, vol. 2, no. 1, pp. 5-15.

- LEMENKOVA, P. 2020b. Variations in the bathymetry and bottom morphology of the Izu-Bonin Trench modelled by GMT. In *Bulletin of Geography. Physical Geography Series*. 2020, vol. 18, no. 1, pp. 41-60.
- LEMENKOVA, P. 2020c. GMT Based Comparative Geomorphological Analysis of the Vityaz and Vanuatu Trenches, Fiji Basin. In *Geodetski List*. 2020, vol. 74, no. 1, pp. 19-39.
- LEMENKOVA, P. 2020d. R Libraries {dendextend} and {magrittr} and Clustering Package `scipy.cluster` of Python for Modelling Diagrams of Dendrogram Trees. In *Carpathian Journal of Electronic and Computer Engineering*. 2020, vol. 13, no. 1, pp. 5-12.
- LEMENKOVA, P. 2019a. Automatic Data Processing for Visualising Yap and Palau Trenches by Generic Mapping Tools. In *Cartographic Letters*. 2019, vol. 27, no. 2, pp. 72-89.
- LEMENKOVA, P. 2019b. Geomorphological modelling and mapping of the Peru-Chile Trench by GMT. In *Polish Cartographical Review*. 2019, vol. 51, no. 4, pp. 181-194.
- LEMENKOVA, P. 2019c. Topographic surface modelling using raster grid datasets by GMT: example of the Kuril-Kamchatka Trench, Pacific Ocean. In *Reports on Geodesy and Geoinformatics*. 2019, vol. 108, pp. 9-22.
- LEMENKOVA, P. 2019d. GMT Based Comparative Analysis and Geomorphological Mapping of the Kermadec and Tonga Trenches, Southwest Pacific Ocean. In *Geographia Technica*. 2019, vol. 14, no. 2, pp. 39-48.
- LEMENKOVA, P. 2019e. Statistical Analysis of the Mariana Trench Geomorphology Using R Programming Language. In *Geodesy and Cartography*. 2019, vol. 45, no. 2, pp. 57-84.
- LEMENKOVA, P. 2019f. AWK and GNU Octave Programming Languages Integrated with Generic Mapping Tools for Geomorphological Analysis. In *GeoScience Engineering*. 2019, vol. 65, no. 4, pp. 1-22.
- LEMENKOVA, P. 2018. R scripting libraries for comparative analysis of the correlation methods to identify factors affecting Mariana Trench formation. In *Journal of Marine Technology and Environment*. 2018, vol. 2, pp. 35-42.
- LEMENKOVA, P. – PROMPER, C. – GLADE, T. 2012. Economic Assessment of Landslide Risk for the Waidhofen a.d. Ybbs Region, Alpine Foreland, Lower Austria. In *Protecting Society through Improved Understanding. 11th International Symposium on Landslides & the 2nd North American Symposium on Landslides & Engineered Slopes (NASL)*. 2012, pp. 279-285.
- MAHONEY, A. R. – EICKEN, H. – GAYLORD, A. G. – GENS, R. 2014. Landfast sea ice extent in the Chukchi and Beaufort Seas: The annual cycle and decadal variability. In *Cold Regions Science and Technology*. 2014, vol. 103, pp. 41-56.
- PAVLIS, N. K. – HOLMES, S. A. – KENYON, S. C. – FACTOR, J. K. 2012. The development and evaluation of the Earth Gravitational Model 2008 (EGM2008).

- In *Journal of Geophysical Research*. 2012, vol. 117, no. B4, pp. 1-38.
- SANDWELL, D. T. – MÜLLER, R. D. – SMITH, W. H. F. – GARCIA, E. – FRANCIS, R. 2014. New global marine gravity model from CryoSat-2 and Jason-1 reveals buried tectonic structure. In *Science*. 2014, vol. 346, no. 6205, pp. 65-67.
- SCHENKE, H. W. – LEMENKOVA, P. 2008. Zur Frage der Meeresboden-Kartographie: Die Nutzung von AutoTrace Digitizer für die Vektorisierung der Bathymetrischen Daten in der Petschora-See. In *Hydrographische Nachrichten*. 2008, vol. 81, pp. 16-21.
- SMITH, W. H. F. 1993. On the accuracy of digital bathymetric data. In *Journal of Geophysical Research*. 1993, vol. 98, no. B6, pp. 9591-9603.
- STEIN, R. 2008. *Arctic Ocean Sediments: Processes, Proxies, and Paleoenvironment*. Amsterdam: Elsevier, 2008. 608 p. ISBN 978-04-445-2018-0.
- STRAUME, E. O. – GAINA, C. – MEDVEDEV, S. – HOCHMUTH, K. – GOHL, K. – WHITTAKER, J. M. – ABDUL FATTAH, R. – DOORNENBAL, J. C. – HOPPER, J. R. 2019. GlobSed: Updated total sediment thickness in the world's oceans. In *Geochemistry, Geophysics, Geosystems*. 2019, vol. 20, no. 4, pp. 1756-1772.
- SUETOVA, I. A. – USHAKOVA, L. A. – LEMENKOVA, P. 2005a. Geoinformation mapping of the Barents and Pechora Seas. In *Geography and Natural Resources*. 2005, vol. 4, pp. 138-142.
- SUETOVA, I. A. – USHAKOVA, L. A. – LEMENKOVA, P. 2005b. Geocological Mapping of the Barents Sea Using GIS. In *International Cartographic Conference (ICC)*. 2005, La Coruna, Spain.
- USHER, P. J. 2002. Inuvialuit Use of the Beaufort Sea and Its Resources, 1960-2000. In *Arctic*. 2002, vol. 55, no 1, pp. 18-28.
- WESSEL, P. – SMITH, W. H. F. 1991. Free software helps map and display data. In *Eos Transactions of the American Geophysical Union*. 1991, vol. 72, no. 41, pp. 441.
- WESSEL, P. – SMITH, W. H. F. 1996. A Global Self-consistent, Hierarchical, High-resolution Shoreline Database. In *Journal of Geophysical Research*. 1996, vol. 101, pp. 8741-8743.
- WESSEL, P. – SMITH, W. H. F. – SCHARROO, R. – LUIS, J. F. – WOBBE, F. 2013. Generic mapping tools: Improved version released. In *Eos Transactions American Geophysical Union*. 2013, vol. 94, no. 45, pp. 409-410.

Polina Lemenkova, MSc.

College of Marine Geo-sciences

Ocean University of China

238 Songling Rd, 266100 Laoshan, Qingdao, People's Republic of China

E-mail: pauline.lemenkova@gmail.com